Published in final edited form as:

Biochim Biophys Acta Proteins Proteom. 2021 February ; 1869(2): 140576. doi:10.1016/j.bbapap.2020.140576.

Detection of key sites of dimer dissociation and unfolding initiation during activation of acid-stress chaperone HdeA at low pH

Marlyn A. Widjaja[1,2], **Jafaeth S. Gomez**[1,2], **Jonathon M. Benson**[1], **Karin A. Crowhurst**[1,*]

[1]Department of Chemistry and Biochemistry, California State University Northridge, 18111 Nordhoff St. Northridge CA 91330-8262

[2]Present address: Amgen, 1 Amgen Center Dr. Thousand Oaks, CA 91320

Abstract

HdeA is a small acid-stress chaperone protein with a unique activity profile. At physiological pH, it forms a folded, but inactive, dimer. Below pH 3.0, HdeA unfolds and dissociates into disordered monomers, utilizing exposed hydrophobic patches to bind other unfolded proteins and prevent their irreversible aggregation. In this way, HdeA has a key role in helping pathogenic bacteria survive our acidic stomach and colonize our intestines, facilitating the spread of dysentery. Despite numerous publications on the topic, there remain questions about the mechanism by which HdeA unfolding and activation are triggered. Previous studies usually assessed HdeA unfolding over pH increments that are too far apart to gain fine detail of the process of unfolding and dimer dissociation, and often employed techniques that prevented thorough evaluation of specific regions of the protein. We used a variety of heteronuclear NMR experiments to investigate changes to backbone and side chain structure and dynamics of HdeA at four pHs between 3.0 and 2.0. We found that the long loop in the dimer interface is an early site of initiation of dimer dissociation, and that a molecular “clasp” near the disulfide bond is broken open at low pH as part, or as a trigger, of unfolding; this process also results in the separation of C-terminal helices and exposure of key hydrophobic client binding sites. Our results highlight important regions of HdeA that may have previously been overlooked because they lie too close to the disulfide bond or are thought to be too dynamic in the folded state to influence unfolding processes.

Keywords

NMR chemical shifts; NMR relaxation experiments; acid-stress protein; chaperone protein; protein unfolding; conditionally disordered protein

*Corresponding author. karin.crowhurst@csun.edu. Phone: 1-818-677-4288.

CRediT author statement:

Marlyn Widjaja: Investigation, Visualization, Formal analysis, Writing – Review and Editing. **Jafaeth Gomez**: Investigation, Formal analysis, Writing – Review and Editing. **Jonathon Benson:** Investigation, Formal analysis. **Karin Crowhurst**: Conceptualization, Funding acquisition, Supervision, Project administration, Investigation, Formal analysis, Visualization, Writing – Original Draft, Writing – Review and Editing.

Introduction

The World Health Organization estimates that the pathogenic bacteria *Escherichia coli, Shigella flexneri* and *Brucella abortus* are responsible for at least 120 million cases of dysentery and over one million deaths each year, with the majority of cases in developing countries with poor sanitation and contaminated water [3]. All three strains have evolved the ability to survive for several hours at extremely low pH [4], due primarily to the presence of HdeA and HdeB, small ATP-independent chaperone proteins found in the periplasm of these bacteria. There is a clear inverse correlation between the ability to survive highly acidic environments and the dose required to infect the host: dysentery is induced with very small quantities of *Shigella*, while infection by *Salmonella* (which does not carry the HdeA / HdeB genes) requires much larger doses [5, 6].

The mode of action of HdeA in its role as a periplasmic chaperone runs against the canonical understanding of protein function, in that it is inactive in its homodimeric folded state at neutral pH (Figure 1) and becomes activated only when it unfolds in the acidic conditions of the stomach [4]; in this manner, HdeA falls into the category of conditionally disordered proteins [7]. Due to the porous outer membrane of gram-negative bacteria, drastic changes in the pH of the surrounding environment cause a corresponding rapid change in the pH of the periplasmic space, followed by a substantial increase in chloride ion concentration (to ~0.6 M) [8]. Thus, periplasmic proteins are far more exposed to changes in environmental conditions compared to cytoplasmic proteins and are consequently far more likely to unfold and/or aggregate after these sudden changes in pH and salt concentration [8–10]. Within this environment, HdeA can bind a variety of periplasmic proteins, protecting them from aggregation and preventing misfolding as the bacteria travel through the stomach towards the higher pH environment of the intestines [4, 5, 11–13]. By the time the bacteria enter and commence infection of the intestinal tract (at neutral pH), HdeA has released these proteins and refolded into its inactive dimer conformation [14].

Not only is it important to understand the mechanism of HdeA activation as a possible therapeutic target to weaken the effectiveness of these pathogenic bacteria, but HdeA is also an interesting and valuable model system to use in efforts to better understand protein folding pathways and triggers of unfolding. Several studies have indicated that exposure to low pH causes HdeA to only partially unfold – exposing key hydrophobic residues that interact with client proteins [4, 14–16]. Recent reports have also attempted to map those client binding sites on activated HdeA [1, 2]. Although HdeA may become activated at slightly higher pHs in the presence of a client protein [1], understanding protein activation in the absence of the client is also valuable, as it highlights the possible routes of unfolding and exposure of hydrophobic clusters that HdeA undergoes in order to bind the client.

Previously, our group provided clear evidence that neutralization of ionizable acidic side chains glutamate and aspartate was not sufficient to trigger unfolding, because HdeA starts unfolding at approximately pH 2.5, which is significantly lower than the ionization pHs, whose lowest pK_a is 3.66 for D20 [17]. We have also shown through hydrogen-deuterium exchange experiments and MD simulations that the N- and C-termini engage in transient but stable interactions at low pH which appear to expose, and provide access to, at least one of

the proposed client binding sites on HdeA [2, 18]. Those experiments have highlighted how valuable it is to monitor HdeA at small (~0.2 unit) pH increments as we approach the unfolded state. Our research and the efforts of others continue to shed light on the mechanism of unfolding and activation of HdeA. However, more work is required to further investigate trigger points of HdeA unfolding at low pH. In this paper we expand our understanding by showing that unfolded state conformations are observed on side chains at higher pHs than are observed on the backbone, highlighting the early loss of structure in specific areas of the protein that aid in the exposure of the hydrophobic core. Our results additionally suggest that there is an interrelated process by which localized increases in dynamics may ultimately trigger unfolding and exposure of client binding sites via the opening of a "clasp" region near the disulfide bond in HdeA.

Results and Discussion

Evidence for the presence of alternate stable conformers in the backbone of HdeA at low pH

Starting at pH 2.8 (and enhanced at pH 2.6) we observe extra backbone peaks in the ^{15}N-HSQC, specifically at residues 3 – 10, 87 and 89 (see Figure S1 for examples). These extra resonances overlay with peaks for those residues in the dominant conformational ensemble of the unfolded state spectrum at pH 2.0, showing that even though the N-terminus is thought to be disordered in the folded state, it still exchanges slowly with a different set of disordered conformations in the unfolded state.

One challenge to studying HdeA in its unfolded monomeric state at pH 2.0 is that numerous additional peaks are observed in the ^{15}N-HSQC, further complicating a spectrum that is highly overlapped due to the narrow range of $^{1}H_N$ chemical shifts. Problems dealing with this complicated spectrum was one reason that Yu et al. utilized their F28W mutant as a substitute [2]; by replacing a phenylalanine in the dimer interface with a tryptophan the authors argued that the monomers are forced apart at low pH. However, this simplified spectrum only occurs in the higher-concentration mixed-buffer conditions at pH 1.5; remarkably, we found that the F28W mutant is in slow exchange between folded and unfolded states at pH 2.0 in citrate buffer, similar to what is seen for wild type HdeA at pH 2.4 (Figure S2). Despite the problem of additional peaks in the wild type we were able to identify 82/84 of the assignable backbone amides at pH 2.0. Interestingly, the two backbone peaks that remain unassigned belong to residues with charged basic side chains (K70 and K75), which also lie in the arguably important proposed "clasp" region (see later discussion), suggesting that they are involved in intermediate timescale motions that broaden their resonances in the ^{15}N-HSQC at low pH.

At pH 2.0 we were also able to assign extra peaks for residues K11, V13, A36, E37, A38, D76, I85 and K86. They do not cluster to a single location on the folded structure, but they may cluster together in the partially unfolded state at pH 2.0. The extra peaks do not have any consistent type (some are hydrophobic, some charged or polar), and it should be noted that there are at least 14 additional "extra" peaks in the ^{15}N-HSQC at pH 2.0 that remain unassigned.

There has been disagreement about whether the extra peaks correspond to residues in an unfolded dimer or just alternative conformations of the unfolded state in slow exchange. Yu et al. argue that they correspond to a dimeric form of unfolded HdeA based on results from gel filtration chromatography [2]. Although it is difficult to picture how an unfolded dimer could exist, there is some support for this possibility in our dynamics data: the average R_2 value for the monomeric protein is 5.8 s^{-1} compared to 9.9 s^{-1} for the extra peaks (see section on protein dynamics, below). Given that R_2 values are impacted by molecular size, this higher average for the extra peaks could be due to a larger molecular weight (from a dimer). In addition, Salmon et al. determined that the self-dissociation constant of HdeA to be 64 μM at pH 2.3 [19], a value that is at least 10-fold lower than the concentration used for these NMR studies; at NMR concentrations, it is therefore possible to have a dimer population (even if it is transient) at pH 2.0. MD simulations performed by Ahlstrom et al. also indicate the feasibility of an “on-pathway” dimeric intermediate with one partially folded monomer [20]. On the other hand, it also conceivable that the extra peaks in the NMR spectrum at pH 2.0 have higher R_2 values due to intermediate conformational exchange and not dimerization. This latter argument is supported by the fact that the average R_2 for the extra peaks at pH 2 is quite a bit lower (~10 s^{-1}) than the average R_2 (~14 s^{-1}) for residues in the folded dimer at higher pHs.

Concentration-dependent presence of unfolded state seen in studies of HdeA backbone at pH 2.6, but not other pHs

When performing our NMR experiments at pH 2.6 it became apparent that the peak content in the ^{15}N-HSQC spectrum varies, depending on the sample concentration. Specifically, at higher NMR concentrations (above approximately 1.0 mM) the spectrum visually resembles that of a dimeric folded protein, while at lower NMR concentrations (~0.5 mM) the spectrum resembles the mixture of folded and unfolded states observed at pH 2.4 (see Figure S3). The difference between what is observed at pH 2.6 versus 2.4 is that at pH 2.6 the proportion of folded : unfolded peaks can be altered as a function of protein concentration, whereas at pH 2.4 that ratio is relatively unaffected by changes in concentration (within the range of concentrations used for NMR). Interestingly, the extra backbone peaks observed at the N-and C-termini (described in the previous section and shown in Figure S1) are present even at high concentrations of HdeA at pH 2.6.

This concentration-dependent phenomenon is not apparent at other acidic pHs (2.0, 2.4, 2.8, 3.0). Thus, HdeA has a unique profile at pH 2.6, as it is part of the gateway between folded and unfolded states: at higher protein concentrations its equilibrium strongly favors the folded state, while at lower concentrations the ratio of folded and unfolded states is close to 50:50. It is important to note that the structural and dynamic properties of the folded state at pH 2.6 do not change as a function of concentration (Figure S4). Since the folded state is our focus at pH 2.6, dynamics experiments were performed solely on NMR samples at concentrations above 1.0 mM in order to eliminate overlap from unfolded state peaks and thereby simplify analysis.

Unfolding transition is observed for the side chains at a higher pH than seen for the backbone

Although assignment of side chain methyls was relatively straightforward for HdeA at pHs 3.0 and 2.8, we encountered a problem at lower pHs, in that the chemical shift changes were drastic and TOCSY experiments could not provide unambiguous assignments. As a result, we turned to assignment by mutagenesis for some unfolded state side chains. The segment of the spectrum associated with leucine and valine methyls is quite crowded at lower pHs; we therefore decided to focus on the isoleucine δ-methyls, which are isolated, less overlapped and considered feasible for analysis via dynamics experiments. It was important to perform mutations that are as conservative as possible; mutations to alanine are frequently highly disruptive. In this case, alanine is significantly smaller than isoleucine and therefore likely to create a void within the hydrophobic core that might alter HdeA structure (and shift peaks). As a result, we created I55V, I62L and I85V mutants of HdeA to aid with chemical shift assignment. With these mutants we were able to assign all isoleucine δ-methyls associated with pHs 2.0, 2.6 and 2.8 (Figure 2a – c).

Despite the success obtaining these assignments we discovered additional challenges with assigning and analyzing the side chain methyl region of the ^{13}C-HSQC at these low pHs. Although the backbone resonances of the folded state in the ^{15}N-HSQC spectra at pHs 2.8 and 2.6 overlay well, and both overlay closely with the folded state spectrum at pH 2.4, the story is different for the side chains. Focusing on the isoleucine region of the ^{13}C-HSQC for selectively δ-methyl-labeled Ile residues, the spectrum at pH 2.8 has three peaks corresponding to the three Ile residues in HdeA (shown in black, Figure 2a) which overlay with the peaks seen at higher pHs (not shown). However, a significant change is observed at pH 2.6 (Figure 2b): although the same three peaks are present as are seen at the higher pHs, four to five additional resonances are observed in that region of the spectrum. By overlaying the spectra at pH 2.6 and 2.4 as well as 2.4 and 2.0, it is clear these new peaks correspond to the unfolded state (Figure 2a – c). This phenomenon is also observed for the resonances corresponding to valine and leucine methyls (Figure 2d – f). It is noteworthy that there are at least five peaks for the three Ile δ-methyls at pH 2.0, indicating multiple stable conformers for the isoleucine methyls in the unfolded state of HdeA (Figure 2c).

In evaluating the methyl region of ^{13}C-HSQC spectra at these pHs and at a range of HdeA concentrations, we also observe that there is some concentration-dependence on the intensities of the unfolded state side chain peaks at pH 2.6: they are more intense (and have better definition) at lower HdeA concentrations at that pH (Figure S5) but (unlike what is seen along the backbone) they are still clearly present at high protein concentrations. There is little, if any, concentration dependence on what is observed at pH 2.0, or at pH 2.8 and higher.

The side chain tryptophan ε1 positions for W16 and W82 also display evidence for slow exchange between unfolded and folded state conformations (Figures 3 and S6). Additional peaks are very weakly present in some spectra at pH 3.0, somewhat weak at pH 2.8, and fairly well-defined by pH 2.6. At pHs 2.8 and 2.6 (regardless of the HdeA concentration we tested) a set of at least four peaks can be observed for W16, and at least two for W82: one for the folded state of each tryptophan and at least one peak for unfolded state conformers.

At pH 2.0, the folded state peaks are gone but the same unfolded state peaks are present (Figure 3). This is consistent with previous ^{19}F work on Trp mutants; in the study by Zhai et al. [21], three additional peaks are also observed for ^{19}F-labeled W16 at pH 2.5, and one additional peak is observed for W82. In unmodified HdeA, we observe that, at low pH, W16 and W82 each have at least one side chain amine peak (W82u and W16u1) with a $^{1}H_{N}$ chemical shift of ~10.1 ppm, which is typical for a fully unfolded protein [22]. However, W16 also has two upfield-shifted peaks (u2 and u3), suggesting that two major conformations of unfolded state HdeA have residual interactions, and possibly residual ring stacking interactions. In the folded state the W16$^{\varepsilon 1}$ peak is very upfield shifted compared to W82$^{\varepsilon 1}$, consistent with the existence of ring stacking interactions at W16, as seen in the crystal structure (see Figure S7) [11]. It should be noted that the crystal structure is used as a reference here to determine side chain positioning in the folded state because the positions of the aromatic side chains in the NMR structure vary so widely in the two chains of the dimer [1], providing some uncertainty about how many NOESY restraints were used to define side chain structure. In the unfolded state, the u2 peak of W16$^{\varepsilon 1}$ is only slightly upfield of the u1 peak, while the u3 peak of W16$^{\varepsilon 1}$ is about halfway between u1 and the folded state position. These peak positions suggest that the indole is in slow exchange between three conformations with varying levels of residual interactions at low pH (u1 being the least structured and most exposed, u3 with the most residual structure and some solvent protection), consistent with the findings by Zhai et al. [21]. Given that the C-terminal region of the protein shows a loss of secondary structure at pH 2.0 (Figure 4), the observation of only one unfolded peak for W82$^{\varepsilon 1}$, at a chemical shift associated with random coil-like conformation at low pH, is expected. Although the side chain amine of W16 has some solvent protection above pH 3 [17], our hydrogen-deuterium exchange experiments show that neither indole amine is well-protected from solvent at or below pH 3 (data not shown); however, CLEANEX-PM experiments, which monitor transient solvent protection [23], show that the folded state of W16 and the u3 conformer of W16 are protected after a 450 ms mixing time (even at pH 2.0, in the case of W16u3) while the other conformers are not (Figure S8).

What is particularly noteworthy about these observations is that the side chain methyls and the aromatic rings of W16 and W82 are, of course, mostly buried in the core of the folded protein. In order to have slow exchange between folded and unfolded conformations for these hydrophobic side chains at a particular pH *without* seeing extensive exchange between folded and unfolded states of the entire protein, HdeA would have to sample backbone conformations that permit greater movement within the core of the protein. This emphasizes the continuing and significant loosening of the structure of HdeA with decreasing pH, in advance of widespread unfolding. With hydrogen-deuterium exchange experiments we previously argued that, at and below pH 2.8, the “inner” core of the folded state structure is increasingly exposed to solvent [18], while residues in the “outer” core were loosened between pHs 6.0 and 3.0. These data support the argument, since the W16 side chain is part of that inner core of hydrophobic residues. Disruption of residues in the inner core of the protein is the next stage in the process of dismantling the stable folded structure, which begins at much higher pHs, as observed previously [17]. Some of the conformational exchange of the residues with side chain methyls is also reflected in the backbone CEST

experiments performed by Yu et al. [2], but those experiments did not detect conformational exchange in either tryptophan.

Chemical shifts are used to highlight changes between folded and unfolded states

We used our chemical shift assignments of HdeA between pHs 3.0 and 2.0 to perform a careful assessment of the changes in secondary structure propensity (SSP) [24] between the folded and unfolded states of HdeA (Figures 4 and S9). In the folded state of the NMR structure [1], helices in HdeA are found at 18 – 22 (A), 28 – 40 (B), 52 – 69 (C) and 75 – 85 (D). In the unfolded state (at pH 2.0), if we count helical propensity as having values of SSP > 0.3 (which is an ensemble average for each residue), there is a modification of the positioning and length of helices: 19 – 25 (A), 39 – 49 (B) and 61 – 65 (C). This is similar to the ranges provided by Yu et al. when analyzing their F28W mutant at pH 1.5, except that they identify a segment near the C-terminus as helical even though the SSP values are very low [2]. Our data show that there is relatively little helical content present at positions beyond residue 68, suggesting that there is little, if any, secondary structure content in the region formerly occupied by helix D, consistent with simulations [20] and hydrogen-deuterium exchange experiments, which show this region has very poor solvent protection at lower pHs [18].

It was also worthwhile to do a deeper evaluation of the chemical shift differences (CSD or Δδ) in HdeA taking place between pH 3.0 (the representative of the folded state) and pH 2.0 (unfolded state), to gain insight into changes in structure and/or chemical environment as HdeA becomes activated. While almost all peaks corresponding to each residue undergo significant shift (average of 0.41 ppm for $^{1}H_{N}$ and ^{15}N combined) there are some residues and regions whose peaks undergo shifts that are far above the average. Figure 5 illustrates the positions of significant chemical shift changes mapped onto the structure of the folded dimer, and Figure S10 provides a plot of Δδ values as a function of residue. Four regions of the protein are worth highlighting here. First, residues E46, A48, L50 and D51 in the BC-loop have notable shift changes, most likely because they lose interactions with residues in the N-terminal region of the other protomer in the dimer as the protein unfolds and the dimer dissociates (Figure 5a and b). Although the D51 side chain is neutralized above the pHs monitored here, there may be some residual interactions (such as hydrogen bonding) with its important binding partner at K10 [16]. Second, A61 (at the center of helix C), has one of the highest CSD values due, most likely, to the loss of interactions with what was formerly helix D (which appears to be eliminated in the unfolded state, Figure 4). A61 experiences the largest change in chemical shift upon unfolding compared to other residues in helix C because it has the closest contact with helix D (Figure 5c): the CA-CA distance between A61 and E81 is 5.8 Å compared to >7 Å for all other contacts. The third region of note surrounds the group of residues C18, A61, V63, C66, Q68, D69, Q71 and A72, all of which are in close proximity to the disulfide bond (Figure 5a and 5d) and undergo notable chemical shift changes (>1.0σ) upon unfolding. This trend is somewhat strange: since the disulfide bond remains intact, one might expect that this region would experience the least structural change and therefore lower chemical shift perturbation. Although they maintain their secondary structure (Figure 4), the CSD results (Figures 5 and S10) and the dynamics data (see below) provide evidence that these segments may undergo a shift, rotation, or other type

of separation from each other (while still tethered by the intact disulfide bond). The final region of interest relates to the residues with by far the largest chemical shift changes: N14 and T17, which are close to Q71 and F74 (Figure 5d). More about this region will be discussed with the dynamics data (below).

Dynamics experiments and methods used for analysis

In order to monitor the loosening of tertiary structure immediately before and during unfolding in addition to the flexibility of the unfolded state, several types of relaxation experiments were performed, including R_1 and R_2 as well as CPMG relaxation dispersion experiments on backbone amides, side chain methyl groups (of isoleucine, leucine and valine amino acids) and side chain tryptophan amines. While the backbone experiments permit us to probe motions at almost every residue in the protein, the side chain methyl and Trp amine experiments are also valuable to monitor changes that occur specifically in the hydrophobic core of the protein under conditions just above the unfolding pH (as has already been illustrated in looking at slow exchange between conformations, discussed above). Previous studies used CEST to study backbone conformational exchange at pHs 4.0, 3.5, 3.0 and 2.5 [17]. CEST is a vehicle to show the proportion of unfolded state character at pHs where the protein appears to be folded. However, its success relies on an observable difference in chemical shift between the folded and unfolded states for a given residue [25], and as a result there may be additional residues exchanging between folded and unfolded states at these pHs that are not detectable by CEST if the ^{15}N CSD is too small. There is a good match between residues with CEST contributions and residues with higher than average chemical shift changes between pHs 2.6 and 2.0 (Figures S10 and S11). This supports the idea that these are regions that undergo changes in chemical environment [2], likely due to structural changes, but it does not necessarily indicate regions at pH 2.5 that have more exchange between folded and unfolded states than other regions.

Considering that CEST monitors relatively slow exchange (in the ms-s range), and we have already reported on conformational dynamics in the min – hour range through hydrogen-deuterium exchange experiments [18] it made sense to additionally perform experiments that would cover the ~0.1 – 10 ms range (CPMG) as well as the broader ps-ns and μs-ms timescales provided by R_1 and R_2 experiments [25]. Although we would have liked to utilize data from experiments recorded at pH 2.4 (the pH at which we observe full sets of both folded and unfolded state peaks), it was decided to exclude those data because the reporting would be incomplete due to extensive overlap in the center of the spectrum. As discussed in our previous publication (and illustrated by the similarity of the pH 2.6 spectrum at lower HdeA concentrations to the pH 2.4 spectrum), data from pH 2.0 and 2.6 appear to be close stand-ins to 2.4u and 2.4f (the unfolded and folded states at pH 2.4), respectively [18].

Typically, one would evaluate standard relaxation data obtained by calculating R_2/R_1 ratios for each residue. However, Kneller et al. have shown that the R_2/R_1 analysis is not able to distinguish between the effects of motional anisotropy and chemical exchange (R_{ex}) [26, 27]. Given the shape of the HdeA dimer, the possible exchange between monomer and dimer at some lower pHs, and the heterogeneous nature of the unfolded state structure, it is not surprising that HdeA might exhibit some motional anisotropy. By taking the product of R_1

and R_2 (R_1R_2) instead, τ_c is no longer a factor; as a result, we are able to clearly and unambiguously identify not only sites of fast (ps-ns) timescale motion (indicated by low R_1R_2 values), but additionally R_{ex} (μs-ms) motions (designated by high R_1R_2 values) which can only be inferred by R_2/R_1 values [26]. By calculating R_1R_2 these areas of high conformational exchange are clear (Figure S12).

Gains and losses in backbone and side chain dynamics paint a picture of several key regions in the unfolding process

Figure 6 provides a summary of the key results from the dynamics experiments we recorded. BMRB entry 50421 and Tables S1 – S3 contain the numbers obtained from the dynamics experiments at pHs 2.8, 2.6 and 2.0, Figure S12 provides the plots of the R_1R_2 backbone data and sample fits to raw CPMG data are shown in Figure S13. We were able to obtain both backbone and methyl side chain data at pHs 6.0, 3.0, 2.8 and 2.6, and backbone but not methyl side chain for pH 2.0 (due to the assignment and overlap challenges enumerated above). When it became apparent that aromatic interactions (especially involving the two tryptophans in HdeA) may be important in our analyses, we also obtained R_1, R_2 and CPMG data for the side chain ε1 amine of tryptophan at pHs 2.8, 2.6 and 2.0. A backbone or side chain position was determined to have fast (ps-ns) motions if R_1R_2 is at least 1.5σ below the mean (excluding 10 % outliers), while R_1R_2 values at least 1.5σ above the mean indicate residues with intermediate (μs-ms) timescale motions (and are not a result of rigidity as has been stated previously for HdeA [2]). For relaxation dispersion experiments, the cutoffs for notable CPMG values were 3 s^{-1} and 4 s^{-1}, respectively, for backbone and side chain motions in the folded state (at pHs 3.0, 2.8 and 2.6), and 6 s^{-1} for backbone and side chain motions in the unfolded state (at pH 2.0).

It is important to assess the change in dynamics in transitioning from the folded state dimer (represented at pH 2.6 and above) to the unfolded state monomer (represented at pH 2.0). As one might expect when moving to a disordered (and presumably more flexible) state at low pH, there are several places in HdeA where an increase in backbone dynamics is observed. This includes Q53, I55, A56, T57 and V58 (Figure 6), which reside in a region of the protein that shows a notable loss in secondary structure content: SSP analysis shows that HdeA loses almost all of the helical structure in the N-terminal half of helix C (Figure S9), probably because that region interacts with helix D in the folded protein (Figure 4). The structure of helix D is also lost, possibly when it becomes untethered from the rest of the protein due to the release of a “clasp” connection between N14 and F74 (see next section).

Of equal, if not greater, interest is to note the regions of unfolded HdeA that *lose* dynamics compared to the folded state. This includes the region comprising L39, N40, K44 and L50, which is found in the segment of the protein that contains the new, shifted position of helix B compared to its position in the folded structure (Figure 4). The combination of decreased dynamics in this region and higher helical propensity for residues 48 – 50 support the idea that this is a new, semi-stabilized secondary structure that forms at low pH. Other segments in which backbone dynamics decrease are at the N- and C-termini. These regions are understood to be unstructured even at high pHs and there is significant evidence that their high charge content is important to the stability and chaperone function of the unfolded state

[1, 4, 15]. However, it was previously reported that there is increased solvent protection at the termini at low pH [18], and in our current experiments we observe a decrease in the number of N-terminal residues with fast timescale dynamics and an elimination of observable dynamics at the C-terminus in the unfolded state (Figure 6). This is consistent with the recently published MD modeling that indicates the N- and C-termini may have increased contacts at low pH, which could therefore lower the dynamics in those regions [18].

Loss of a clasp-like interaction may be essential to unfolding and exposure of client binding sites

One very important region of change in dynamics is found between residues 13 – 15 (before helix A) and 74 (in the loop before helix D), which are directly across from each other in the folded protein (see Figure 5d). They exhibit significant intermediate timescale dynamics in the folded state but become less dynamic in the unfolded state (Figures 6 and S12). This, combined with the fact that residues N14 and T17 (the latter of which is directly across from F74) show the highest chemical shift change upon unfolding (Figure S10), suggests that these two segments of the protein (broadly encompassing residues 13 – 17 and 71 – 74) act like a “clasp” at higher pHs, which springs open as part of the unfolding process or as a trigger of unfolding (Figure 7). It should be noted that residues in these two regions become significantly less protected from solvent in transitioning from pH 3.0 to 2.8 [18], and residues 73 – 76 undergo a sharp decrease in secondary structure propensity below pH 3.0 (Figure S9); thus, the loosening of this clasp connection is already in progress before the protein formally unfolds. This is also supported by the appearance of unfolded state peaks for hydrophobic residues at about pH 2.8 (Figures 2 and 3), suggesting that the hydrophobic core is being transiently exposed before the clasp is fully broken.

Although more work and modeling may be needed to fully understand the ultimate trigger of clasp breakage, some possible sources have already been identified. In our previous work we saw evidence for increased sampling of interactions between the N- and C-termini as the pH is lowered [18]. Given that the termini are not within normal contact range in the folded state (even the N- and C-termini of opposite protomers of the dimer are separated by >11Å), these novel interactions put strain on long-range contacts such as the clasp region and may therefore weaken the interactions between clasp residues. The aromaticity of F74 may also play a role in this clasp activity. In the folded state the side chains of W16 and F74 as well as F21 and F74 (but not W16 and F21) can engage in π-stacking interactions (since they are <4 Å apart in the crystal structure, see Figure S7). Zhai et al. found that mutating F21 or F74 caused HdeA to unfold at a higher pH, so it is clear these interactions are important for stabilizing the folded structure [21]. Although the backbone of F74 participates in intermediate timescale motions between pH 6.0 and 2.6, the side chain interaction can still be stably maintained. However, at pH 2.0 the backbone of F21 engages in intermediate timescale dynamics for the first time while F74 loses those dynamics; this disruption may help explain the separation of these two regions of the protein that are part of the clasp and the likely exposure of the hydrophobic core of the monomer [18].

Along with F21, surrounding residues 18 – 23 (within helix A) and 63 – 67 (within helix C) gain dynamics in the unfolded state – this is a clear change of the key regions of intermediate timescale R_1R_2 dynamics compared to the folded state (at residues 13 – 15 and 74 – 76) (Figure S12). Additionally, it should not be forgotten that the side chain δ-methyl of I62 undergoes conformational exchange between at least 3 conformers in the unfolded state (Figure 2). Residues 18 – 23 and 63 – 67 are across from each other in the folded protein and, given their proximity to the disulfide bond, are almost certainly close in the unfolded state as well. Interestingly, these segments lie on the opposite side of the intact disulfide from the clasp region. It is possible that the loss of the clasp interaction frees this area to increase movement, but the fact that these are intermediate and not fast timescale motions indicates that the region is still somewhat restricted by the presence of the disulfide.

Model of some key elements of dissociation and unfolding

In looking at our results, we propose a low-pH model of HdeA unfolding that highlights one key site of dimer dissociation and another of unfolding initiation (Figure 7). Significant intermediate conformational exchange in the long BC-loop (residues 41 – 51) at pH 6 is consistent with alternating interactions with both the N-terminal residues as well as residues in the BC-loop region of the other protomer in the dimer [1, 11, 28]. Dimer separation may begin in this region, as seen by intermediate timescale motions moving down the loop toward helices B and C at pH 2.8 (Figure 7a) and supported by activation mechanisms proposed by other groups [2, 21]. At pH 2.6 all intermediate timescale motion in the BC-loop is gone, and there is evidence for fast timescale motion at the tip (Figure 6), illustrating the separation of the BC-loop from the dimer interface as well as fewer contacts with the N-terminal residues. Although the change in secondary structure propensity in helix B and the BC loop does not occur until the protein unfolds at low pH (Figures 7b and S9) the process of loop disengagement from the dimer interface and loss of contacts with the N-terminus of the other protomer is started at much higher pHs.

Between pH 6.0 and 2.6 we see intermediate timescale motions at residues 14, 15 and 17, along with 73 – 75 directly opposite in the folded structure. It is unclear what role intermediate timescale dynamics might have in this region when HdeA is in its folded inactive state, but these motions are eliminated (or significantly decreased) at pH 2.0. Combined with large chemical shift changes in some of these residues upon unfolding, the data point to a severing of long-range contacts between these two regions at low pH, consistent with the opening of a metaphorical clasp. Separation of these segments fully exposes the hydrophobic core and client binding sites of HdeA, especially client binding site II which was identified by Yu et al. [2] (Figure 7c); this process may therefore be a crucial step in the activation of the chaperone, and warrants continued study. In looking at the changes in secondary structural propensity as a function of pH (Figure S9) we see that residues 73 – 76 in the clasp region lose secondary structure below pH 3.0, while the loss of any residual structure of the N-terminal half of helix C and all of helix D occurs only when the protein becomes unfolded at low pH. Although we cannot yet be certain of the order of events, the data suggest that the opening of the clasp region pushes helix D away from HdeA, and the loss of the stabilizing interactions between helices C and D triggers the loss of secondary structure. However, there are several previously published simulations that

suggest unfolding in HdeA is initiated at the helix D [20, 29, 30], so we cannot rule out the possibility that the loss of structure at helix D triggers the clasp opening. In fact, some of our data support the idea that residues in the region of 13 – 17 may remain in place while the other side of the clasp is pulled away: one unfolded state conformation of the indole amine at W16 maintains some solvent protection at pH 2.0 (Figure S8), and the backbone amide of V13, which is positioned directly across from the W16 amine in the folded state, is still protected from solvent in hydrogen-deuterium exchange experiments for at least an hour at pH 2.0. Future experiments will be aimed at clarifying this order of events.

We also observe intermediate timescale motions appearing near the N-terminus and decreased fast timescale motions at the C-terminus at pH 2.6, which are eliminated by pH 2.0. This is consistent with MD simulations which show evidence that the N- and C-termini of each protomer transiently interact with each other, exposing a proposed client binding site at residues 49 – 55 [2, 18]. This interaction may be one major contributor to the breakage of the clasp interaction, since its formation would create strain in other parts of the molecule, especially impacting long-range interactions.

Taken together, these results point to the BC loop region, which helps to peel the monomers apart, as well as the C-terminal helix and a clasp-like region near the disulfide bond in HdeA that change as the pH is gradually decreased, all of which are proposed to be key elements that lead to HdeA unfolding, dimer dissociation and chaperone activation as access to different hydrophobic client binding sites is facilitated (Figure 7).

Materials and Methods

Isotopes were obtained from Cambridge Isotope Laboratories, and chromatography columns were from GE Lifesciences.

Preparation of HdeA

HdeA was prepared as outlined previously [17, 18, 31]. Briefly, HdeA was expressed in minimal medium in BL21(DE3) *E. coli* at 37 °C. For samples that were uniformly ^{15}N or $^{15}N/^{13}C$-labeled, the minimal medium contained ^{15}N ammonium chloride and/or ^{13}C glucose and 5% (v/v) $^{15}N/^{13}C$ BioExpress rich medium supplement. In cases where the protein was selectively labeled, ^{13}C methyl-labeled amino acid precursors α-ketoisovalerate and α-ketobutyrate were also added to the culture, at concentrations of 125 mg/L and 75 mg/L, respectively, 1 hour prior to induction [32]. For selectively labeled samples the amount of BioExpress was decreased or eliminated to avoid incorporating amino acids with undesirable labeling schemes. After a three-hour induction period, the cell pellet was treated with buffer containing polymyxin B sulfate to extract the contents of the periplasm, and HdeA was purified via pH gradient on a cation exchange column, followed by polishing using a size exclusion column. Typical yields of HdeA were 12 mg protein from 1 L culture for uniformly labeled samples, and 5 mg/L for selectively labeled samples.

Site-directed mutagenesis was executed using the QuikChange Lightning kit from Agilent. Expression and purification of mutants was performed in the same manner as for the wild type (outlined above).

NMR experiments

HdeA samples were prepared for NMR through dialysis into 50 mM citrate buffer at the desired pH, except for experiments recorded at pH 1.5, which utilized a buffer mixture of 50 mM sodium phosphate and 45 mM citrate. The pH meter was calibrated before each use and the buffers were regularly checked with a different pH probe and meter to ensure accuracy. NMR samples for peak and chemical shift analysis had protein concentrations in the range of 0.5 – 1.2 mM, while protein concentrations for relaxation experiments were 1.0 – 1.2 mM.

NMR data were obtained at 25 °C on an in-house Agilent DD2 600 MHz spectrometer with a triple resonance probe. For some experiments we also utilized a Varian VNMRS 800 MHz NMR spectrometer at NMRFAM (UW Madison) equipped with a cryogenic probe, or a Varian VNMRS 800 MHz NMR spectrometer with a room temperature probe at the University of Connecticut Health Sciences Center. All raw data were processed using NMRPipe/NMRDraw [33, 34] and the resulting spectra were viewed and analyzed using NMRViewJ [35, 36]. Most assignment and dynamics data have been deposited at BMRB, entry 50421. Data for “extra” peaks and CPMG are provided in the supplemental materials.

Chemical shift assignment - backbone.—Backbone chemical shift assignment of HdeA at pHs 2.6 and 2.8 required only HNCaCb and CbCa(CO)NH experiments, while assignment of HdeA at pH 2.4 required HNCaCb, CbCa(CO)NH as well as HNCO and HN(Ca)CO spectra to resolve and assign both folded and unfolded backbone peaks. In many cases the data from pH 2.6 were used to aid assignment of the folded peaks at pH 2.4. Assignment of HdeA at pH 2.0 was achieved, in part, by assigning the mutant HdeA-F28W at pH 1.5 [2]. Experiments for assignment of HdeA-F28W included HNCaCb, CbCa(CO)NH, HNCO, HN(Ca)CO and HNN [37] spectra. Most peaks from the mutant could be mapped onto the spectrum of the wild type at pH 2.0, and the data were also used to help assign the unfolded peaks at pH 2.4. Additional assignments of the backbone of wild type HdeA at pH 2.0 (for peaks not present in the spectra for the HdeA-F28W mutant) were made using HNCaCb and CbCa(CO)NH experiments.

Chemical shift differences (CSDs, or Δδ) for HdeA between pH 3.0 and 2.0 were calculated using the equation:

$$\Delta\delta = \sqrt{\frac{(\Delta H)^2 + \left(\frac{\Delta N}{7}\right)^2}{2}}$$

where ΔH and ΔN refer to the differences in backbone $^{1}H_N$ and ^{15}N chemical shifts between pH 3.0 and 2.0 for a given residue. ΔN is scaled so that chemical shift changes in each dimension of the ^{15}N-HSQC are weighted similarly.

Secondary structure propensity.—SSP analysis was performed on HdeA using H_N, N, Cα and Cβ chemical shifts for data obtained at each pH [24].

Chemical shift assignment – side chain.—Side chain assignment of methyl groups of isoleucine, leucine and valine utilized HCC-TOCSY-NH, CCC-TOCSY-NH and HCCH-TOCSY experiments at pHs 3.0 and 2.8 if assignments could not be made from following peak movements with decreasing pH. However, the chemical shift changes became more drastic and additional peaks (corresponding to the unfolded state) appeared at and below pH 2.6, preventing the acquisition of unambiguous assignments from the TOCSY experiments. As a result, we attempted assignment by mutagenesis for the unfolded state. The segment of the spectrum associated with leucine and valine methyls is quite crowded at lower pHs; we therefore decided to focus on the isoleucine δ-methyls, which are isolated and less overlapped (and thus more likely to produce results from dynamics experiments).

Assignments of Hε1 and Nε1 atoms on tryptophan side chains were achieved using a NOESY-^{15}N-HSQC experiment recorded at pH 2.6: the assignments of folded state ε1 peaks had already been obtained [31] and since the unfolded state peaks are also visible at pH 2.6, we took advantage of the fact that there is conformational exchange between the folded and unfolded states of the sidechain amines and used the patterns of NOESY crosspeaks from the folded state to assign unfolded state peaks for side chain Trp amines (see Figure S6).

Relaxation experiments.—Backbone R_1 relaxation rates were measured on the 600 MHz spectrometer using relaxation delays of 10 (x3), 50, 100, 150, 200 (x2), 250, 300, 400, 500, 600 and 800 ms and R_2 rates were determined using relaxation delays of 10 (x2), 30 (x2), 50, 70, 90 (x2), 110, 130, 150 and 170 ms (recorded in random order). ^{15}N-^{1}H NOE values, when recorded, were determined from peak intensities in spectra obtained with/without 3 s proton saturation, recorded in duplicate.

^{15}N-CPMG datasets were acquired at both 600 MHz and 800 MHz (except for data recorded between pH 6.0 and 3.0 and at pH 2.0, which were recorded only at 600 MHz) with a constant-time CPMG element of 40 ms. At 600 MHz each pseudo-3D experiment comprised 19 νCPMG values, ranging from 0 to 1000 Hz, with two points repeated for error analysis [38], while the 800 MHz data sets comprised 13 νCPMG values, ranging from 0 to 1000 Hz with one point repeated. ^{13}C-CPMG datasets were acquired at both 600 MHz and 800 MHz (except for data recorded between pH 6.0 and 3.0 and at pH 2.0, which were recorded only at 600 MHz) with constant-time CPMG elements of 20 and 40 ms, respectively. At 600 MHz each pseudo-3D experiment comprised 17 νCPMG values, ranging from 0 to 750 Hz, with two points repeated for error analysis [38], while the 800 MHz data sets comprised 14 νCPMG values, ranging from 0 to 1000 Hz with one point repeated.

R_1, R_2 and ssNOE experiments were analyzed using NMRViewJ software [35, 36] while relaxation dispersion data were analyzed using the GLOVE software package [39]. Figures containing protein structures were rendered using PyMol and figures containing plots were generated using SigmaPlot.

Supplementary Material

Refer to Web version on PubMed Central for supplementary material.

Acknowledgements

We gratefully acknowledge the NIH for research support (SC3-GM116745) and the NSF for funding the purchase of our 600 MHz NMR spectrometer (CHE-1040134). Sincere thanks also go to Marco Tonelli at NMRFAM for his assistance with the setup of our experiments on the 800 MHz spectrometer, and to Irina Bezsonova and Dmitry Korzhnev (UCHC) as well as Ranjith Muhandiram (University of Toronto) for assistance with the setup of the relaxation dispersion and HNN assignment experiments and for helpful discussions. Finally, the authors appreciate the generosity of Dr James Bardwell, who provided us with the HdeA plasmid.

Abbreviations:

CPMG	Carr-Purcell-Meiboom-Gill
CSD or Δδ	chemical shift difference or perturbation
HdeA	HNS (histone-like nucleoid structuring)-dependent expression A
HSQC	heteronuclear single quantum coherence
SSP	secondary structure propensity

References

[1]. Yu XC, Yang C, Ding J, Niu X, Hu Y & Jin C (2017). Characterizations of the Interactions between Escherichia coli Periplasmic Chaperone HdeA and Its Native Substrates during Acid Stress. Biochemistry. 56, 5748–5757. [PubMed: 29016106]

[2]. Yu XC, Hu Y, Ding J, Li H & Jin C (2019). Structural basis and mechanism of the unfolding-induced activation of HdeA, a bacterial acid response chaperone. J Biol Chem. 294, 3192–3206. [PubMed: 30573682]

[3]. Niyogi SK (2005). Shigellosis. J Microbiol. 43, 133–143. [PubMed: 15880088]

[4]. Hong W, Jiao W, Hu J, Zhang J, Liu C, Fu X, Shen D, Xia B & Chang Z (2005). Periplasmic protein HdeA exhibits chaperone-like activity exclusively within stomach pH range by transforming into disordered conformation. J Biol Chem. 280, 27029–27034. [PubMed: 15911614]

[5]. Hong W, Wu YE, Fu X & Chang Z (2012). Chaperone-dependent mechanisms for acid resistance in enteric bacteria. Trends Microbiol. 20, 328–335. [PubMed: 22459131]

[6]. Waterman SR & Small PL (1996). Identification of sigma S-dependent genes associated with the stationary-phase acid-resistance phenotype of Shigella flexneri. Mol Microbiol. 21, 925–940. [PubMed: 8885264]

[7]. Bardwell JC & Jakob U (2012). Conditional disorder in chaperone action. Trends Biochem Sci. 37, 517–525. [PubMed: 23018052]

[8]. Stull F, Hipp H, Stockbridge RB & Bardwell JCA (2018). In vivo chloride concentrations surge to proteotoxic levels during acid stress. Nat Chem Biol. 14, 1051–1058. [PubMed: 30323217]

[9]. Goemans C, Denoncin K & Collet JF (2014). Folding mechanisms of periplasmic proteins. Biochim Biophys Acta - Molecular Cell Research. 1843, 1517–1528.

[10]. Koebnik R, Locher KP & Van Gelder P (2000). Structure and function of bacterial outer membrane proteins: barrels in a nutshell. Mol Microbiol. 37, 239–253. [PubMed: 10931321]

[11]. Gajiwala KS & Burley SK (2000). HDEA, a periplasmic protein that supports acid resistance in pathogenic enteric bacteria. J Mol Biol. 295, 605–612. [PubMed: 10623550]

[12]. Malki A, Le HT, Milles S, Kern R, Caldas T, Abdallah J & Richarme G (2008). Solubilization of protein aggregates by the acid stress chaperones HdeA and HdeB. J Biol Chem. 283, 13679–13687. [PubMed: 18359765]

[13]. Zhang S, He D, Yang Y, Lin S, Zhang M, Dai S & Chen PR (2016). Comparative proteomics reveal distinct chaperone-client interactions in supporting bacterial acid resistance. Proc Natl Acad Sci U S A. 113, 10872–10877. [PubMed: 27621474]

[14]. Tapley TL, Korner JL, Barge MT, Hupfeld J, Schauerte JA, Gafni A, Jakob U & Bardwell JC (2009). Structural plasticity of an acid-activated chaperone allows promiscuous substrate binding. Proc Natl Acad Sci U S A. 106, 5557–5562. [PubMed: 19321422]

[15]. Wu YE, Hong W, Liu C, Zhang L & Chang Z (2008). Conserved amphiphilic feature is essential for periplasmic chaperone HdeA to support acid resistance in enteric bacteria. Biochem J. 412, 389–397. [PubMed: 18271752]

[16]. Foit L, George JS, Zhang BW, Brooks CL 3rd & Bardwell JC (2013). Chaperone activation by unfolding. Proc Natl Acad Sci U S A. 110, E1254–1262. [PubMed: 23487787]

[17]. Garrison MA & Crowhurst KA (2014). NMR-monitored titration of acid-stress bacterial chaperone HdeA reveals that Asp and Glu charge neutralization produces a loosened dimer structure in preparation for protein unfolding and chaperone activation. Protein Sci. 23, 167–178. [PubMed: 24375557]

[18]. Pacheco S, Widjaja MA, Gomez JS, Crowhurst KA & Abrol R (2020). The complex role of the N-terminus and acidic residues of HdeA as pH-dependent switches in its chaperone function. Biophysical Chemistry. 264, 106406. [PubMed: 32593908]

[19]. Salmon L, Stull F, Sayle S, Cato C, Akgul S, Foit L, Ahlstrom LS, Eisenmesser EZ, Al-Hashimi HM, Bardwell JCA & Horowitz S (2018). The Mechanism of HdeA Unfolding and Chaperone Activation. J Mol Biol. 430, 33–40. [PubMed: 29138002]

[20]. Ahlstrom LS, Dickson A & Brooks CL 3rd. (2013). Binding and folding of the small bacterial chaperone HdeA. J Phys Chem B. 117, 13219–13225. [PubMed: 23738772]

[21]. Zhai Z, Wu Q, Zheng W, Liu M, Pielak GJ & Li C (2015). Roles of structural plasticity in chaperone HdeA activity are revealed by ^{19}F NMR. Chem Sci. 7, 2222–2228. [PubMed: 29910910]

[22]. Hausser KH & Kalbitzer HR (1991). NMR Spectroscopy of Biological Macromolecules. In NMR in medicine and biology: structure determination, tomography, in vivo spectroscopy, pp. 75–134, Springer-Verlag, Berlin.

[23]. Hwang T-L, van Zijl PCM & Mori S (1998). Accurate quantitation of water-amide proton exchange rates using the Phase-Modulated CLEAN chemical EXchange (CLEANEX-PM) approach with a Fast-HSQC (FHSQC) detection scheme. J Biomol NMR. 11, 221–226. [PubMed: 9679296]

[24]. Marsh JA, Singh VK, Jia Z & Forman-Kay JD (2006). Sensitivity of secondary structure propensities to sequence differences between alpha- and gamma-synuclein: implications for fibrillation. Protein Sci. 15, 2795–2804. [PubMed: 17088319]

[25]. Anthis NJ & Clore GM (2015). Visualizing transient dark states by NMR spectroscopy. Q Rev Biophys. 48, 35–116. [PubMed: 25710841]

[26]. Kneller JM, Lu M & Bracken C (2002). An effective method for the discrimination of motional anisotropy and chemical exchange. J Am Chem Soc. 124, 1852–1853. [PubMed: 11866588]

[27]. Namanja AT, Peng T, Zintsmaster JS, Elson AC, Shakour MG & Peng JW (2007). Substrate recognition reduces side-chain flexibility for conserved hydrophobic residues in human Pin1. Structure. 15, 313–327. [PubMed: 17355867]

[28]. Zhang BW, Brunetti L & Brooks CL 3rd. (2011). Probing pH-dependent dissociation of HdeA dimers. J Am Chem Soc. 133, 19393–19398. [PubMed: 22026371]

[29]. Dickson A, Ahlstrom LS & Brooks CL 3rd. (2016). Coupled folding and binding with 2D Window-Exchange Umbrella Sampling. J Comput Chem. 37, 587–594. [PubMed: 26250657]

[30]. Socher E & Sticht H (2016). Probing the Structure of the Escherichia coli Periplasmic Proteins HdeA and YmgD by Molecular Dynamics Simulations. J Phys Chem B. 120, 11845–11855. [PubMed: 27787971]

[31]. Crowhurst KA (2014). ^{13}C, ^{15}N and ^{1}H backbone and side chain chemical shift assignment of acid-stress bacterial chaperone HdeA at pH 6. Biomol NMR Assign. 8, 319–323. [PubMed: 23835624]

[32]. Ruschak AM & Kay LE (2010). Methyl groups as probes of supra-molecular structure, dynamics and function. J Biomol NMR. 46, 75–87. [PubMed: 19784810]

[33]. Delaglio F NMRPipe / NMRDraw. 9.6 ed. North Potomac, MD: NMR Science; 2018.

[34]. Delaglio F, Grzesiek S, Vuister GW, Zhu G, Pfeifer J & Bax A (1995). NMRPipe: a multidimensional spectral processing system based on UNIX pipes. J Biomol NMR. 6, 277–293. [PubMed: 8520220]

[35]. Johnson BA NMRViewJ. 9.2 ed. Newark, NJ: One Moon Scientific, Inc.; 2016.

[36]. Johnson BA & Blevins RA (1994). NMR View - A computer-program for the visualization and analysis of NMR data. J Biomol NMR. 4, 603–614. [PubMed: 22911360]

[37]. Panchal SC, Bhavesh NS & Hosur RV (2001). Improved 3D triple resonance experiments, HNN and HN(C)N, for HN and ^{15}N sequential correlations in (^{13}C, ^{15}N) labeled proteins: application to unfolded proteins. J Biomol NMR. 20, 135–147. [PubMed: 11495245]

[38]. Korzhnev DM, Salvatella X, Vendruscolo M, Di Nardo AA, Davidson AR, Dobson CM & Kay LE (2004). Low-populated folding intermediates of Fyn SH3 characterized by relaxation dispersion NMR. Nature. 430, 586–590. [PubMed: 15282609]

[39]. Sugase K, Konuma T, Lansing JC & Wright PE (2013). Fast and accurate fitting of relaxation dispersion data using the flexible software package GLOVE. J Biomol NMR. 56, 275–283. [PubMed: 23754491]

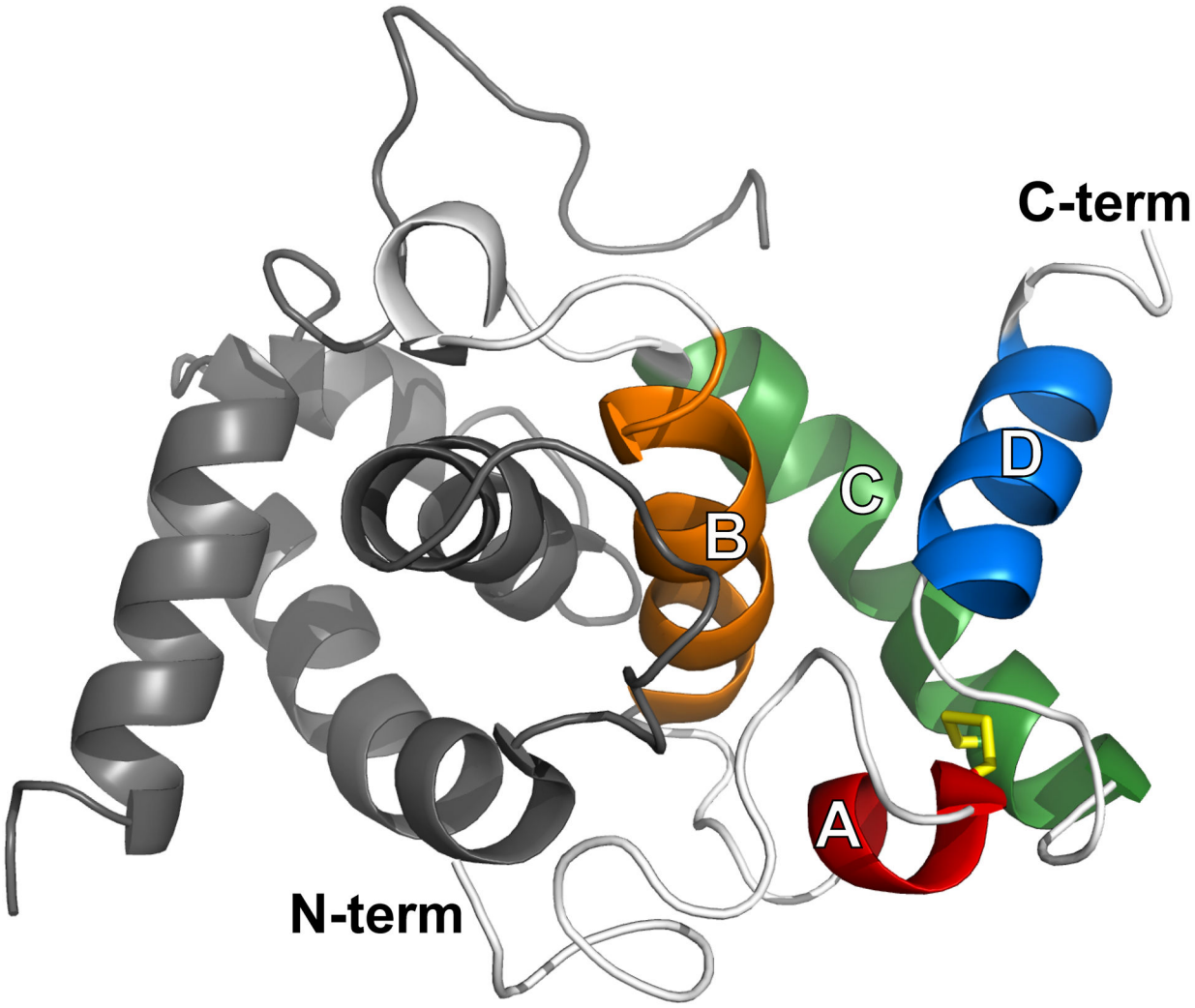

Figure 1.

Labeled structure of the folded HdeA homodimer (PDB ID 5WYO) [1]. In one monomer helix A (residues 18 – 22) is red, B (28 – 40) is orange, C (52 – 69) is green and D (75 – 85) is blue (and labeled with white letters), and the N- and C-termini are labeled with black letters. The disulfide bond between residues 18 and 66 is shown in yellow.

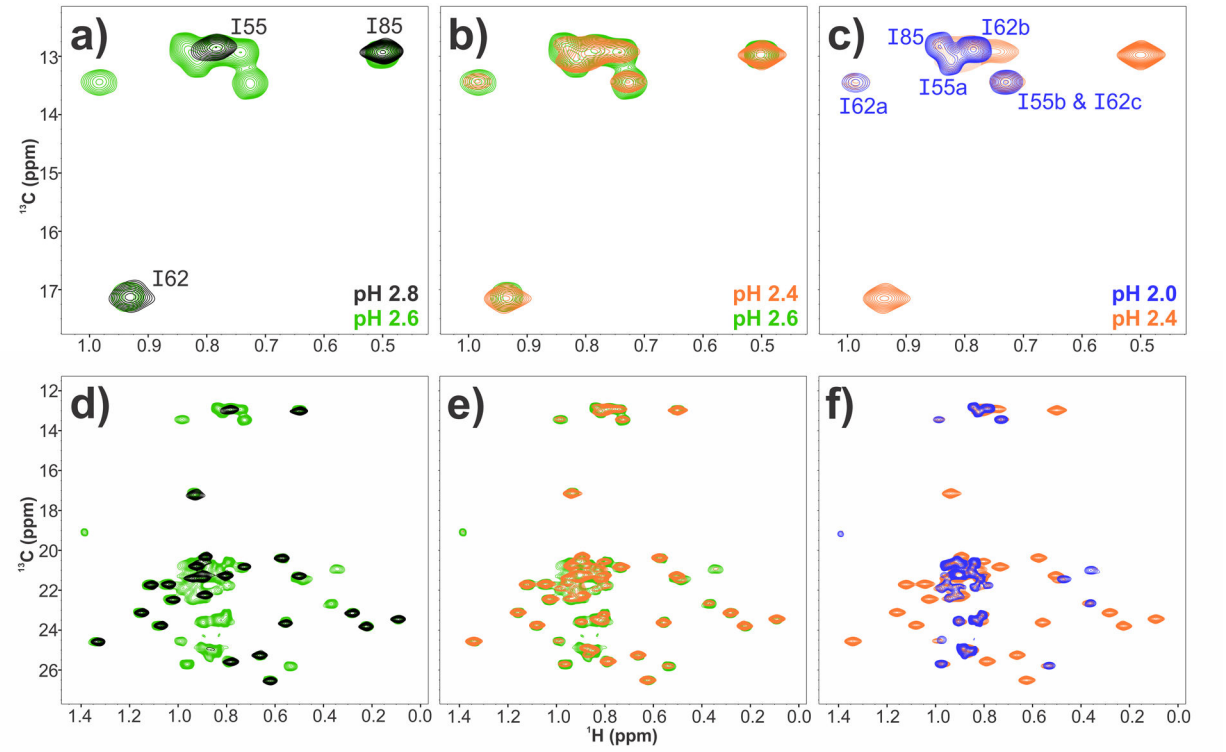

Figure 2.

Methyl region of ^{13}C-HSQC spectra of selectively methyl-labeled HdeA at various pHs. **a – c** show overlays of spectra at different pHs, focusing on the isoleucine δ-methyl groups. **d – f** show overlays of the entire methyl region at different pHs. HdeA spectra were recorded at pH 2.8 (black), 2.6 (green), 2.4 (orange) and 2.0 (blue). Isoleucine peak assignments at pHs 2.8 and 2.0 are shown in **a**) and **c**), respectively.

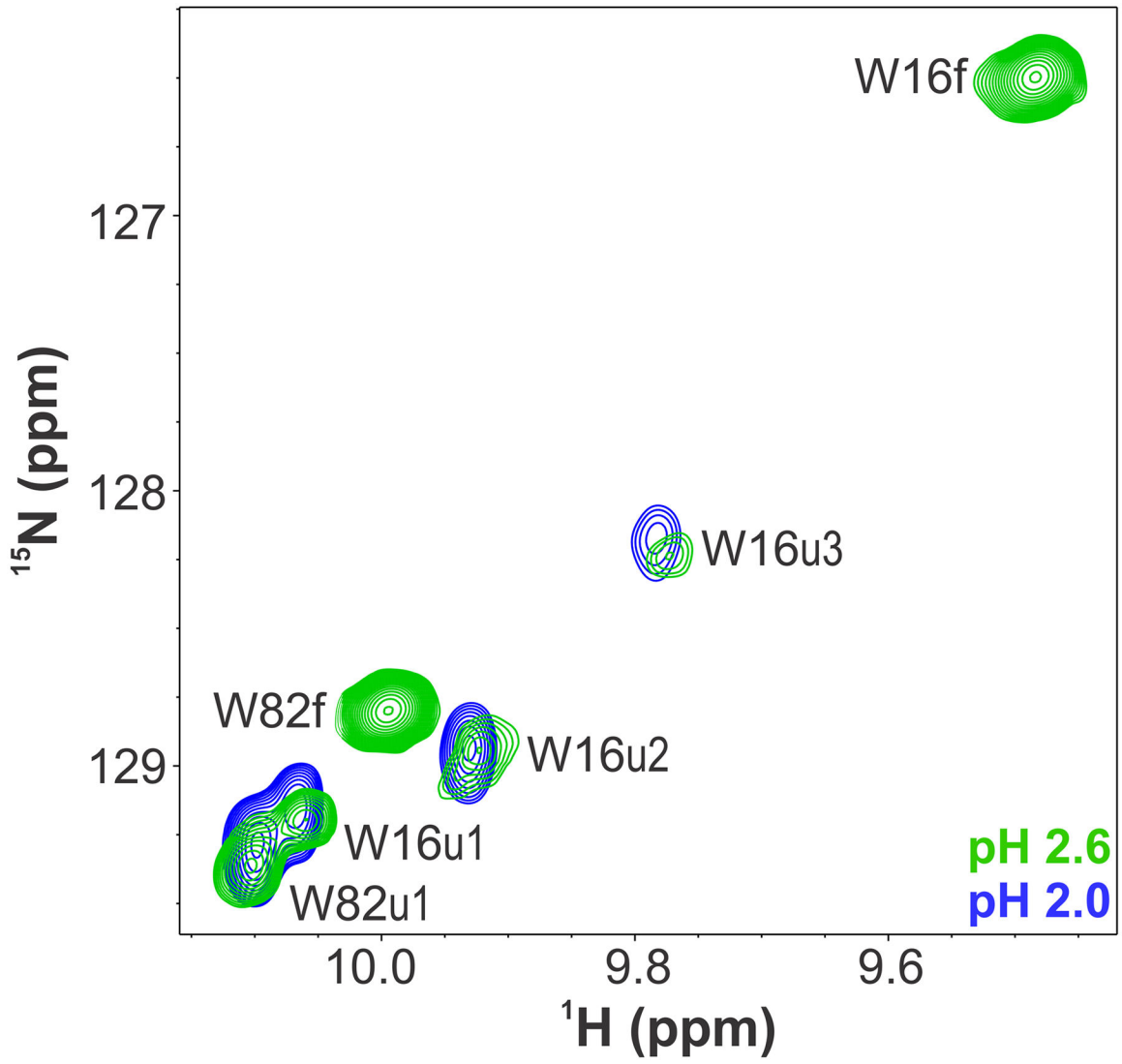

Figure 3.

Segment of ^{15}N-HSQC spectra showing overlay of tryptophan ε1 amines at pHs 2.0 (blue) and 2.6 (green). Peaks designated with “f” and “u” correspond to the folded and unfolded state peaks for each Trp ε1 group, respectively. For W16 the unfolded peaks are numbered.

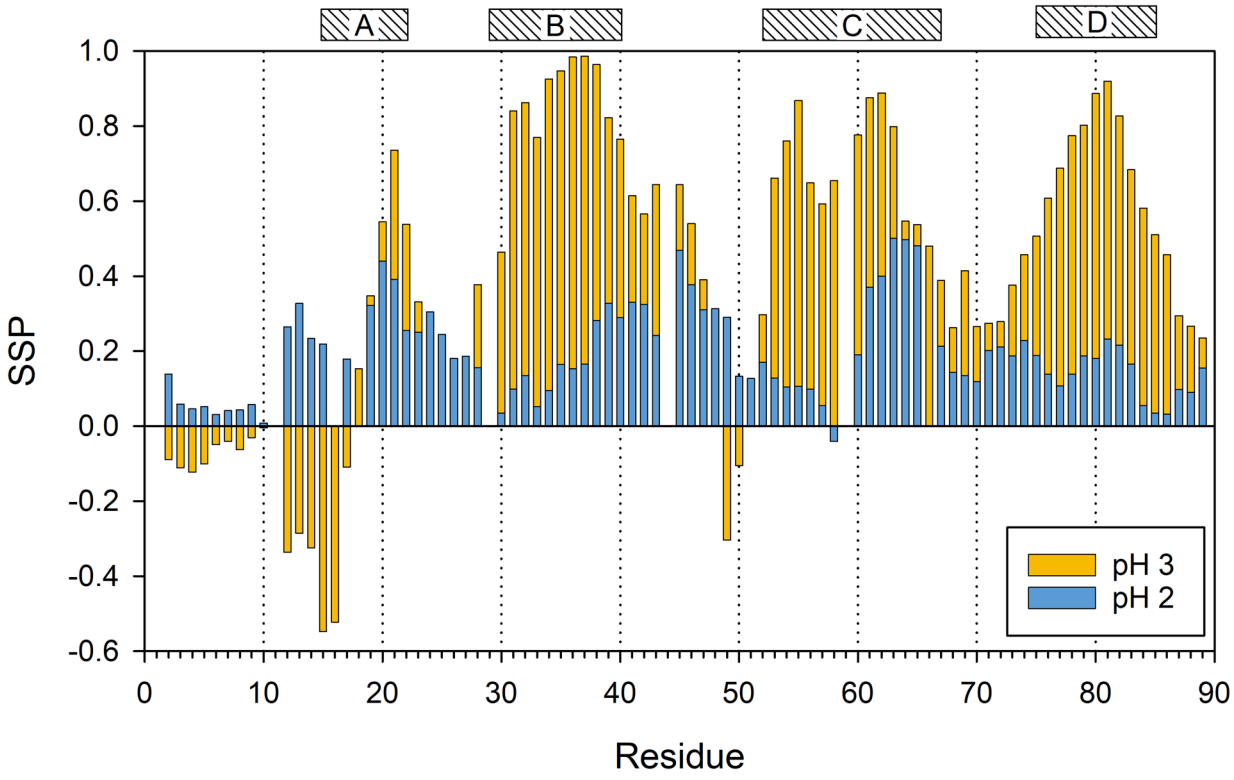

Figure 4.

Overlay of plots of secondary structure propensities (SSP) of HdeA at pH 3.0 (yellow) and 2.0 (blue) as a function of residue number. These numbers have been calculated using H_N, N, Cα and Cβ chemical shifts. Negative numbers indicate β-strand/β-sheet propensity, and the positive numbers indicate α-helical propensity, with greater numbers indicating greater propensity. The position of the helices in the folded state (as determined by the NMR structure 5WYO) [1] are indicated above the graph with hatched rectangles.

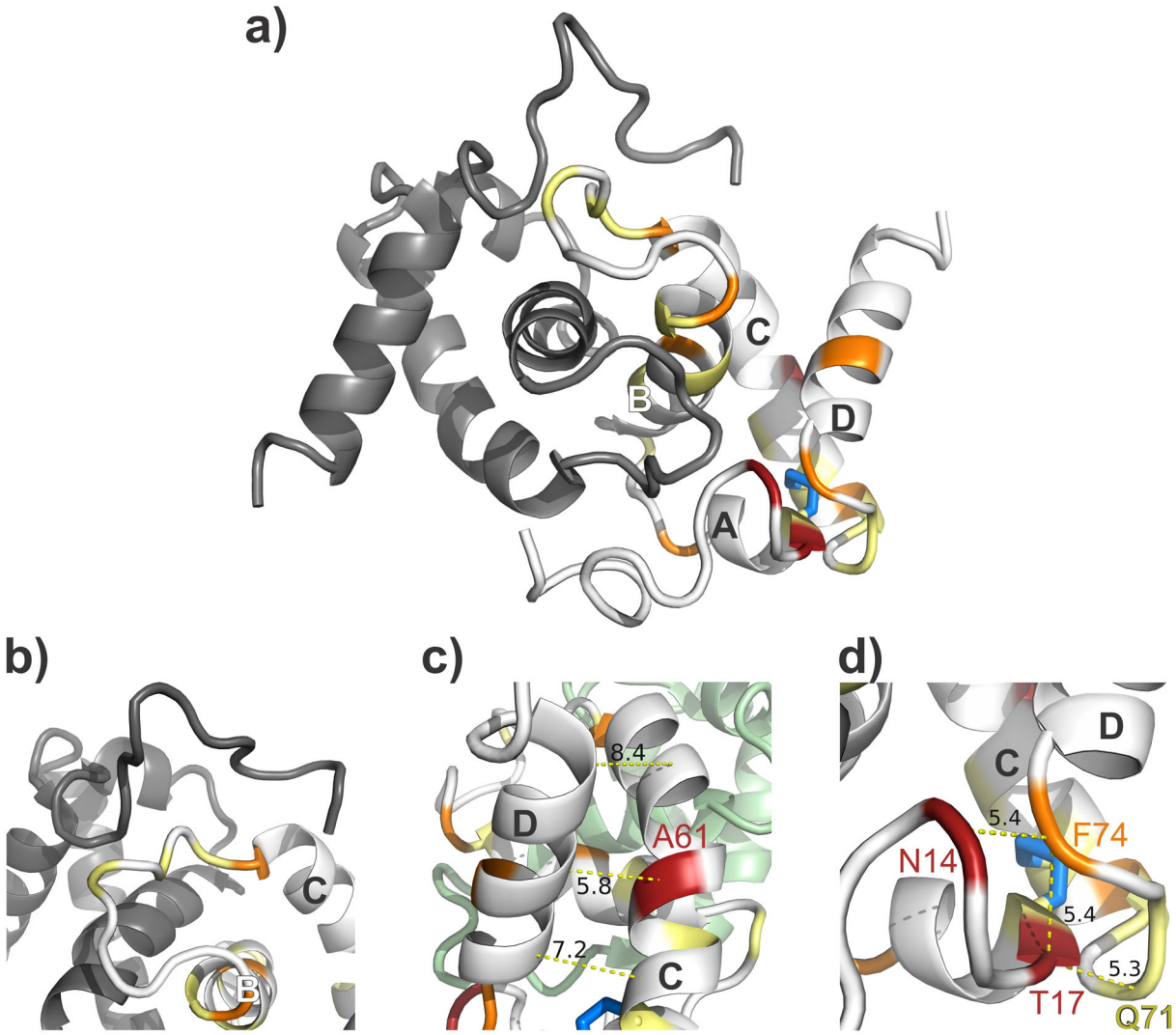

Figure 5.

Significant backbone chemical shift changes (Δδ) for HdeA between pH 3.0 and 2.0, plotted on the folded dimer (PDB ID 5WYO) [1]. **a**) Overview of sites of largest chemical shift changes, plotted on one protomer of the dimer. Three residues with the highest chemical shift change are highlighted in red, while the other residues with Δδ values >1.5σ above the average shift (excluding 10% outliers) are colored orange, and residues whose shifts are between 1.0σ and 1.5σ above average are colored yellow. The second protomer is colored grey, the disulfide is highlighted in blue sticks and helices A – D are labeled. **b**) Enlargement of residues E46, A48, L50 and D51, which have Δδ > 1.0σ, likely reflecting the loss of their interactions with the N-terminus of the other protomer in the dimer as the protein unfolds. **c**) Rotation of the structure in **a**) around the z-axis by ~90° allows for the observation of the closest CA-CA contacts (with distances labeled in Å) between helices C and D, highlighting that A61 is the position in helix C closest to D. **d**) Expansion of region near the disulfide, showing the close contacts between N14 and T17 (the residues with the largest Δδ between the folded and unfolded states) with F74 at the site of the folding clasp.

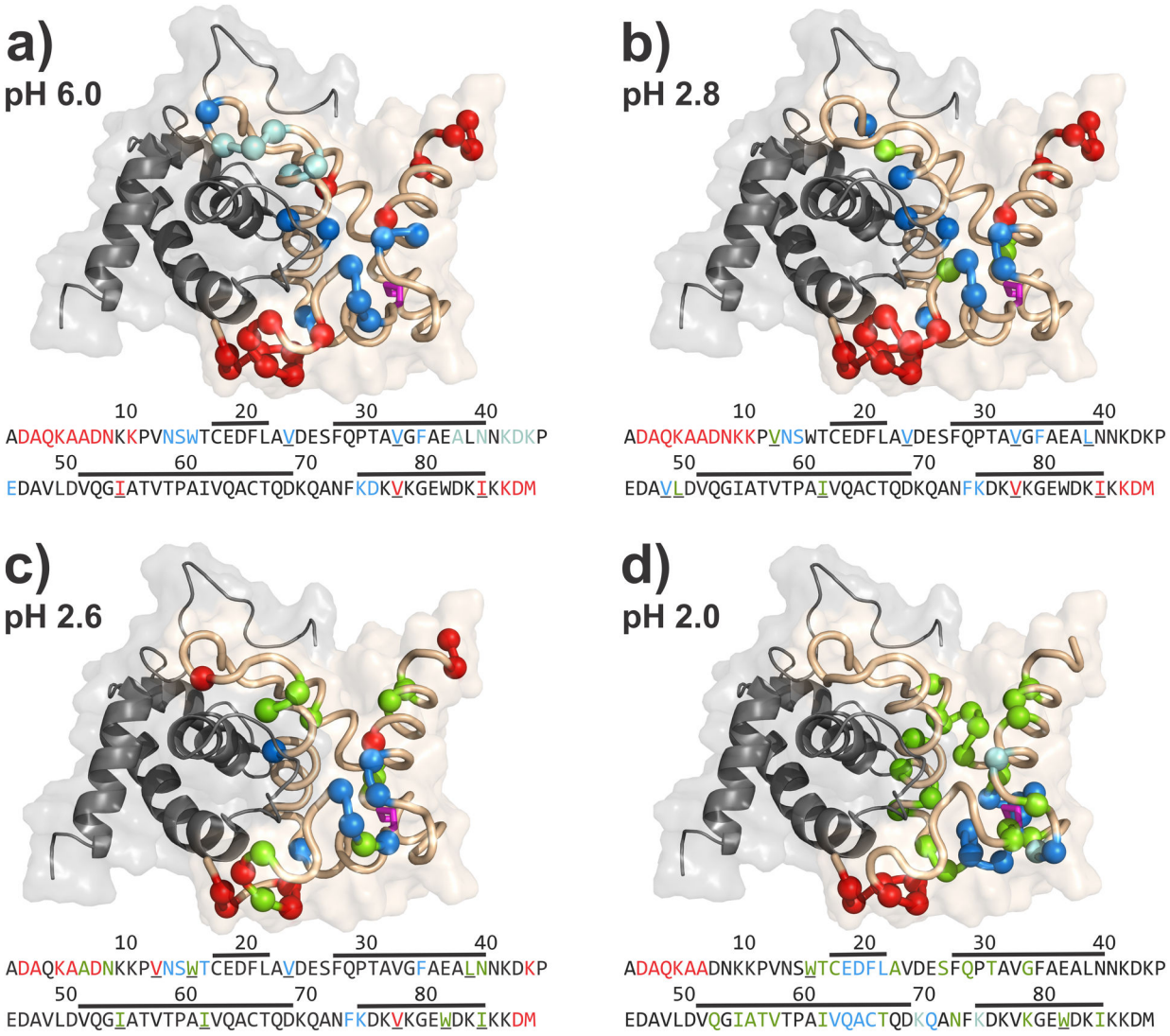

Figure 6.

Dynamics data for HdeA at various pHs, mapped onto the folded dimer structure (PDB ID 5WYO) [1]. Backbone, Trp ε1 and methyl side chain dynamics at **a**) pH 6.0, **b**) pH 2.8 and **c**) pH 2.6. **d**) Backbone and Trp ε1 side chain dynamics at pH 2.0. Red spheres indicate the presence of fast timescale motion at that residue (based on values that are at least 1.5σ below the mean R_1R_2 value (excluding 10% outliers)), blue spheres represent residues with intermediate (μs-ms) timescale motions, obtained from R_1R_2 data (based on values that are at least 1.5σ above the mean (excluding 10% outliers)) and green spheres correspond to residues with intermediate timescale motions measured via CPMG experiments (cutoff of 3 and 6 s^{-1} for backbone motions in folded and unfolded states, respectively, and 4 s^{-1} for side chain motions in the folded state). In cases where a residue displays both fast and intermediate timescale motion the sphere is colored for the latter, and if intermediate timescale motion is observed from both CPMG and R_1R_2 experiments, the position is colored green (corresponding to CPMG). The light blue spheres at pHs 6.0 and 2.0 indicate residues whose backbone peaks are unassigned due to intermediate timescale

conformational exchange dynamics. The protein sequence is provided beneath each structure, color coded as mentioned above. Horizontal lines above the sequences correspond to the location of helices A – D in the folded protein. Lines underneath individual residues indicate that those dynamics data were derived, at least in part, from side chain experiments.

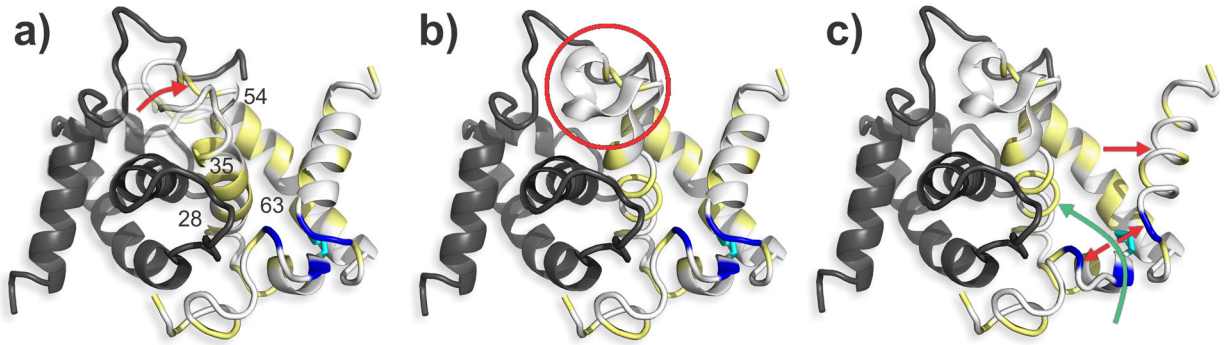

Figure 7.

Model of important stages of HdeA unfolding and access to client binding sites as the pH is decreased, plotted on the folded dimer (PDB ID 5WYO) [1]. Note that these panels do not necessarily indicate a sequential process. **a)** Red arrow indicates movement of BC-loop region away from interactions with the N-terminus of the other protomer. The semi-transparent component indicates the original position of the unaltered loop. The location of hydrophobic residues in HdeA are colored yellow on one protomer in the dimer, while the other protomer is colored uniformly grey. The position of the disulfide bond (C18-C66) is indicated with sticks and colored cyan. The positions of the "clasp" residues (N14, T17, N73 and F74) are colored dark blue. The segment of proposed client binding site II (residues 28 and 35) is labeled,[2] along with another highly hydrophobic region between residues 54 and 63. **b)** Red circle indicates the conversion of the BC-loop to a structure with increased relative helical content at lower pH. Helix B is also shown as loops to indicate a decrease in helical content. **c)** Red arrows indicate the structural separation of the "clasp" residues (N14, T17, N73 and F74) as well as the movement of helix D away from the structure. Helix D is also shown as loops to indicate its loss of helical content. The green arrow illustrates the new access provided to the hydrophobic regions and proposed client binding site as a result of the opening of the clasp region.